Earthquakes and Structures, *Vol. 17, No. 3 (2019) 297-306*
DOI: https://doi.org/10.12989/eas.2019.17.3.297

Seismic behaviour of RC columns with welded rebars or mechanical splices of reinforcement

George I. Kalogeropoulos[1a], Alexander-Dimitrios G. Tsonos[*1] and Dimitrios Konstantinidis[2b]

[1]Department of Civil Engineering, Aristotle University of Thessaloniki, GR-54-124 Thessaloniki, Greece
[2]Department of Civil Engineering T.E., Alexander Technological Educational Institute of Thessaloniki, GR-57-400, Greece

(*Received May 21, 2019, Revised August 2, 2019, Accepted August 9, 2019*)

Abstract. The extension of existing RC buildings is a challenging process, which requires efficient connection between existing and new materials to guarantee load transferring between the lap-spliced longitudinal columns' reinforcement. Therefore, the length of the columns' starter bars is a crucial factor, which decisively affects the seismic response of the new columns. In particular, when the length of the starter bars is short, then the length of the lap splices of reinforcement is inadequate to ensure load transfer between steel bars and concrete, with an indisputable detrimental impact on the seismic behaviour of the columns. Moreover, in most of the existing RC buildings the column starter bars are of particularly short length, while they have probably been bent, cut or corroded. In the present study, the effectiveness of both welded rebar and mechanical splices of reinforcement in ensuring load transferring between the starter bars and the longitudinal reinforcement of the new column was experimentally evaluated. Four cantilever column subassemblages were constructed and subjected to earthquake-type loading. Three of the specimens were used to examine different types of shielded metal arc welding (SMAW), while in the fourth subassemblage mechanical splices were tested. The hysteretic response of the columns was evaluated and compared to the behaviour of a fifth specimen with continuous reinforcement, tested by Kalogeropoulos and Tsonos (2019). Test results clearly demonstrated that the examined types of SMAW were equally satisfactory in ensuring the ductile seismic performance of the columns, while the mechanical splices found to be more susceptible to exhibit slipping of the bars.

Keywords: RC columns; rebar; welding; mechanical splices of reinforcement

1. Introduction

Reinforced Concrete (RC) structures built prior to the 1960-70s possess numerous structural deficiencies, mainly due to lack of capacity design approach, substandard material properties and poor detailing of reinforcement. As a result, these structures are extremely vulnerable during earthquakes and susceptible to developing brittle failure mechanisms, related to catastrophic partial or general collapse (Karayannis and Golias 2018, Chalioris and Bantilas 2017, Karayannis 2015, Kakaletsis *et al.* 2011). Moreover, they are underperforming with respect to modern code requirements. In particular, their hysteresis behavior is dominated by rapid degradation of lateral strength and stiffness, while showing poor energy dissipation capacity and low deformability. The above mainly result from a combination of structural deficiencies, namely the use of plain steel reinforcement, the inadequate length of lap splices of the column reinforcement, the inadequate confinement due to widely spaced transverse reinforcement, the use of concrete with low compression strength.

*Corresponding author, Professor
E-mail: tsonosa@civil.auth.gr
[a]Ph.D.
E-mail: geokal@civil.auth.gr
[b]Professor
E-mail: dkon@cie.teithe.gr

The length of lap splices of reinforcement is a crucial factor, which decisively affects the column cyclic performance (Paulay 1982, Rodriguez and Park 1994, Aboutaha *et al.* 1996, Lynn *et al.* 1996, Daudey and Filiatrault 2000, Pavese *et al.* 2004, Melek and Wallace 2004, Pampanin *et al.* 2007, Kalogeropoulos and Tsonos 2014, 2019). In fact, in structures built prior to the 1960-70s the lap splices of reinforcement were designed for gravity loads only and thus, were very short and insufficient to allow load transfer between the starter bars and the column reinforcement under tension. According to this practice, the length of starter bars left on the top of RC structures was also inadequate. Furthermore, the starter bars on top of existing RC structures are often bent, cut, or/and corroded (Apostolopoulos *et al.* 2008). Consequently, if the vertical extension of pre-1970s substandard RC structures is attempted, the lap splices between the existing starter bars and the new column reinforcement will not satisfy the requirements of modern design codes.

To confront this serious weakness, which adversely affects the seismic behaviour of columns by significantly reducing deformation capacity and flexural resistance, additional measures must be undertaken. According to literature, the most common practice is to provide additional confinement to the lap splice region in favour of improving the bond stresses between steel bars and concrete and prevent premature slipping of the bars (Chai *et al*. 1991, Priestley *et al.* 1996, Aboutaha *et al.* 1999, El Gawady *et al.* 2010, Choi *et al.* 2013). The latter was found to be quite effective in remedying these detrimental effects. However, if the available length of the starter bars is

http://www.techno-press.com/journals/eas&subpage=7 ISSN: 2092-7614 (Print), 2092-7622 (Online)

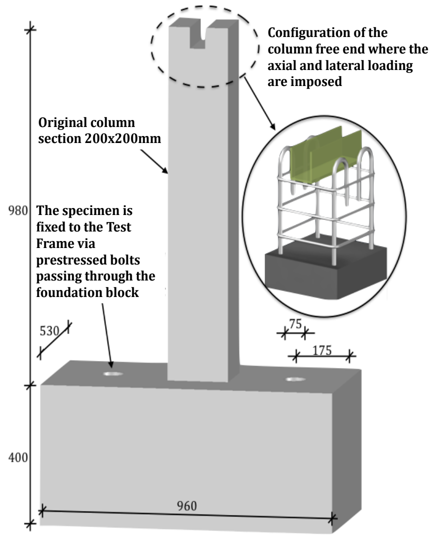

Fig. 1 (a) Dimensions (mm) of the column specimens

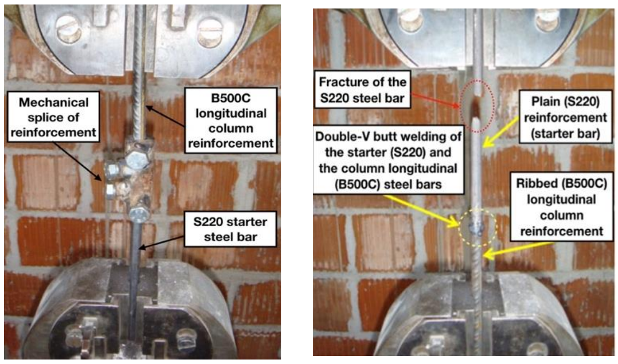

(a) Tensile test-Mechanical splice of steel bars

(b) Tensile test-Fracture of S220 steel bar occurred while the double-V butt welding remained intact

Fig. 2 Tensile tests on the welded rebars and the mechanical splice of reinforcement

extremely short or/and the steel bars are corroded, the lap splice failure can not always be inhibited by providing additional confinement. Alternatively, the load transfer between the starter bars and column reinforcement could be achieved through welding of the rebars or by using mechanical splices of reinforcement (Paulson and Hanson 1991, Issar and Nasr 2006, Se-Jung *et al.* 2013, Haber *et al.* 2014, 2015, Tazarv and Saiid Saiidi 2016). The first however, requires that the steel starter bars are weldable, which must be ascertained though comprehensive chemical analysis. Thereafter, the welding of rebar must conform to rigorous standards, while tensile tests on specimens must also be performed. On the other hand, using mechanical splices of reinforcement requires careful configuration of the mechanical connections (i.e., threaded coupling members, or engineered screwlocks).

2. Experimental program

The ductile seismic behaviour, control of damage and collapse prevention of RC structures are inseparably related to the flexural/shear strength and the ultimate deformation capacity of the columns. After all, low flexural and shear resistance as well as poor ductility of columns were the principal structural deficiencies, which caused catastrophic collapses of numerous pre-1960-70s RC structures during strong earthquake events of the last sixty years worldwide. Along these lines, it was considered of a particular interest to attempt to investigate the efficiency of both welded rebars and of mechanical splices of reinforcement in ensuring load transfer between the starter bars and column reinforcement. Besides, the latter is a crucial factor, which may have a particularly detrimental impact on the seismic behaviour of the columns (Paulay 1982).

An experimental program was conducted for four cantilever column specimens with rectangular cross-section of approximately 1:1.5 scale (see Fig. 1). The specimens were designated as W_1, W_2, W_3 and M_1 and they were used to simulate new columns, constructed for the vertical extension of an existing pre-1960-70s RC structure. Therefore, the foundation block of the columns was constructed with concrete of low compression strength of approximately 10 MPa (see Table 1). Moreover, the starter bars of each column consisted of four S220 plain steel bars with a diameter of 10mm, which were well anchored in the foundation block. The columns were designed to satisfy the requirements of Eurocode 2 and 8 (EC2 and EC8). Thus, the longitudinal reinforcement consisted of four B500C steel bars with a diameter of 10 mm, while the transverse reinforcement consisted of B500C closed hoops of 8mm diameter spaced at 80mm. Furthermore, C20/25 concrete was used for the construction of the columns. Reinforcement details and material properties for each column subassemblage are shown in Table 1.

Prior to the welding of the rebars, chemical analysis on Ø10mm S220 plain steel bars was executed using an optical emission spectrometer. The results of the chemical analysis are presented in Table 2 and showed that the S220 plain steel reinforcement was weldable. The mechanical characteristics of the longitudinal Ø10 mm S220 plain steel bars are shown in Table 3. The efficiency of two different configuration types of welded lap joint (specimens W_1 and W_3) and of the Double-V butt welding of rebars (specimen W_2) were experimentally investigated. In the case of subassemblage M_1 mechanical splices of reinforcement were used to ensure load transfer between the starter bars and the column reinforcement. Meanwhile, tensile tests were also conducted on specimens with welded rebars and with mechanical splice of reinforcement (see Fig. 2). In Fig. 3 reinforcement details of the four columns are depicted, while in Fig. 4 the requirements of CSRTC (2008) for the examined types of welding of the rebars are illustrated.

All columns were subjected to a large number of inelastic cyclic lateral displacements under constant axial loading of 150 kN to simulate the equivalent of strong earthquake motions. The seismic behaviour of specimens W_1, W_2, W_3 and M_1 was compared to that of a control column subassemblage with continuous reinforcement, C_1, which was tested in a previous research work (Kalogeropoulos and Tsonos 2019). The latter was representative of columns found in pre-1960-70s RC

Table 1 Experimental program

Specimen	C_1 (control) (Kalogeropoulos and Tsonos 2019)	W_1	W_2	W_3	M_1
Cross-section dimensions (mm)	200×200	200×200	200×200	200×200	200×200
Column axial load (kN)	150	150	150	150	150
Longitudinal reinforcement	4Ø10 mm S220	4Ø10 mm B500C	4Ø10 mm B500C	4Ø10 mm B500C	4Ø10 mm B500C
Transverse reinforcement	Ø6/200 mm S220	Ø8/80 mm B500C	Ø8/80 mm B500C	Ø8/80 mm B500C	Ø8/80 mm B500C
Steel yield stress (MPa) (longitudinal/transverse)	374 / 263.50	518	518	518	518
Concrete compression strength of columns (MPa)	10.25	21.15 (11.01) ✯	20.58 (10.10) ✯	22.67 (9.22) ✯	19.03 (8.90) ✯
✤Shielded Metal Arc Welding (SMAW)	-	Welded lap joint (type 1*)	Double-V butt	Welded lap joint (type 2*)	-
Mechanical splices of reinforcement	-	-	-	-	Engineered screwlocks

✯Numbers in the parenthesis refer to the concrete compression strength of the foundation block of the column specimens, ✤According to the provisions of CSRTC (2008), * Lap joint type 1 and 2 are illustrated in Fig. 4.

(a) Welded lap joint of reinforcing bars - type 1. Specimen W_1

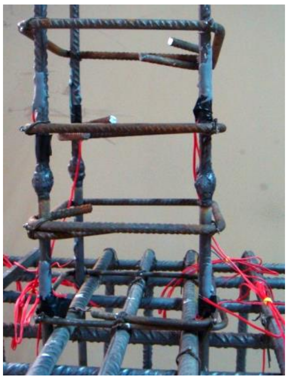

(b) Double-V butt welding of reinforcing bars. Specimen W_2

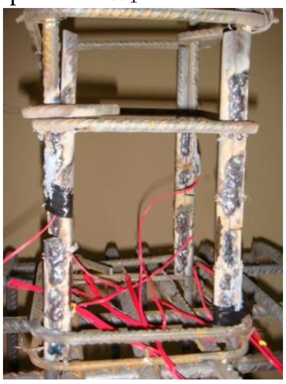

(c) Welded lap joint of reinforcing bars - type 2. Specimen W_3

(d) Mechanical splices of reinforcement (screwlocks). Specimen M_1

Fig. 3 Interventions to ensure load transfer between steel bars and concrete

structures, with concrete of low compression strength equal to 10.25 MPa, S220 plain steel reinforcement and poor reinforcement details (see Table 1). However, the longitudinal reinforcement of C_1 was continuous instead of lap-spliced, to ensure the optimal cyclic lateral performance of a column found in existing substandard RC structures.

Table 2 Results of the chemical analysis on Ø10 mm S220 plain steel bars, executed by optical emission spectrometer

C	0.118
Mn	0.58
P	0.025
S	0.033
Cr	0.13
Ni	0.15
Mo	0.02
V	0
Cu	0.30
N	0.009
Ceq*	0.276

*Equivalent of carbon (maximum acceptable value: 0.52 according to ASTM E 415-08 and ELOT EN 10080-05)

Table 3 Mechanical characteristics of the longitudinal Ø10 mm S220 plain steel bars

	Yield stress (N/mm^2)	Tensile stress (N/mm^2)	Elongation (%)
Ø10 mm S220	374	454	38.3

Thus, test results of specimen C_1 are discussed herein and compared with the results of columns W_1, W_2, W_3 and M_1.

3. Reaction frame and loading sequence

The column specimens were subjected to earthquake-type loading to simulate the equivalent effect of strong earthquakes. Thus, the subassemblages were loaded transversely, under constant axial loading of 150 kN, which permitted easy observation of crack-pattern development. The seismic tests were conducted in the test setup shown in Fig. 5, which is located in the Laboratory of Reinforced Concrete and Masonry Structures of the Aristotle University of Thessaloniki. The structures were fixed to the test frame with post-tensioned bars (see Fig. 5), thus the

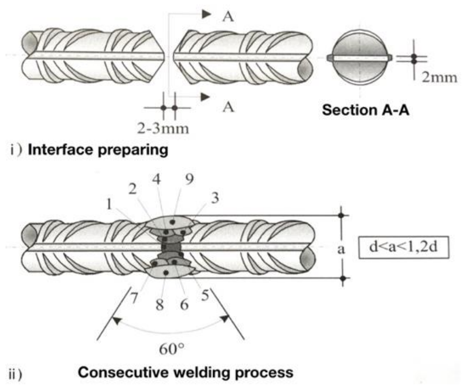

(a) Shielded metal arc welding (SMAW) - Double-V butt welding of reinforcing bars

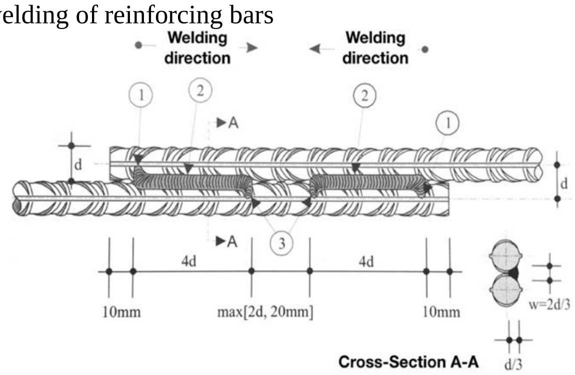

(b) Shielded metal arc welding (SMAW) - Welded lap joint of steel reinforcing bars - type 1

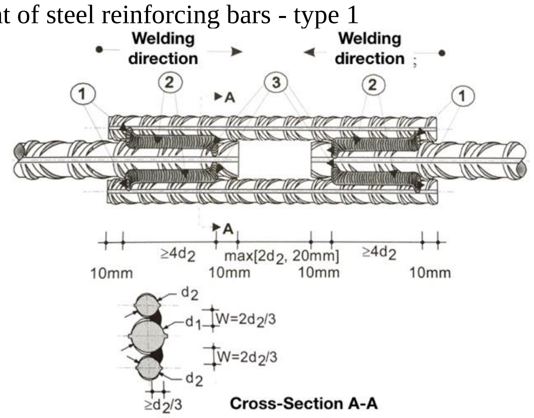

(c) Shielded metal arc welding (SMAW) - Welded lap joint of steel reinforcing bars - type 2

Fig. 4 Requirements of the CSRTC (2008)

horizontal and vertical displacement and the rotation of the foundation block of each column were restrained. A hydraulic jack, placed on top of each column perpendicular to the lateral loading direction, was used to impose the axial load to the specimens and controlled to keep constant during the tests. The lateral loading was applied with a two-way actuator by slowly displacing the column free end of the specimens. The shear resistance of the columns was measured by a load-cell, while a calibrated linear variable differential transducer was used to control the load-point displacement. Electrical resistant strain gauges were installed to the columns' longitudinal reinforcement to measure the steel strain values during the seismic loading and ascertain the yielding of reinforcement. The exact location of each strain gauge is shown in Fig. 12.

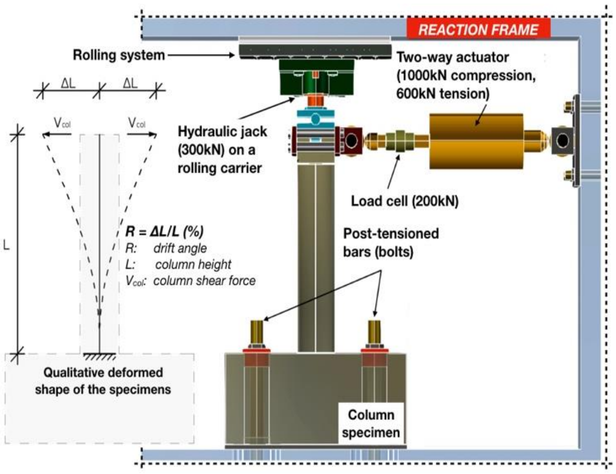

Fig. 5 Details of the test setup and the instrumentation used and qualitative deformed shape of the specimens

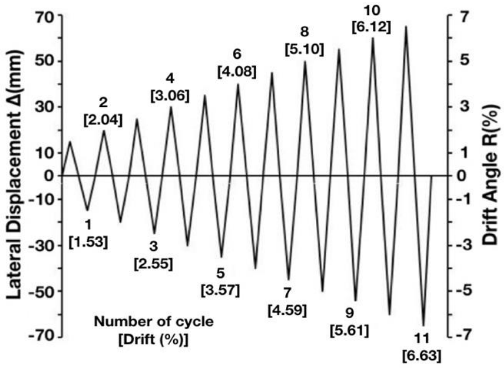

Fig. 6 Lateral displacement history

All specimens were loaded transversely following the displacement-controlled schedule shown in Fig. 6. In Fig. 6 the correspondence of the top displacement amplitudes to the drift angles is also depicted. The seismic loading sequence was established to capture critical issues of the element capacity, for instance the ultimate limit state of the column. Given that the inelastic cyclic deformations cause cumulative damage and that the behaviour of subassemblages is mainly demonstrated by the envelope curves, a sequence with constantly increasing lateral displacement per step and with one cycle per amplitude of displacement was adopted, without considerable influence in the seismic performance of the subassemblages. An original specimen was used to determine the steps of loading and was at first loaded to its yield displacement. This was measured from the plot of applied shear-versus-displacement of the specimen for the point when a significant decrease in stiffness occurred and was also verified by the yielding of the longitudinal column reinforcement. The loading was continued in the same direction (push cycles) to 1.5 times the yield displacement and the subassemblage was subsequently loaded in the other direction (pull cycles) to the same lateral displacement. After the first cycle of loading, the maximum displacement of each subsequent cycle was increased incrementally by 0.5 times the yield displacement (Hakuto *et al.* 2000, Ehsani and Wight 1985, Durani and Wight 1987).

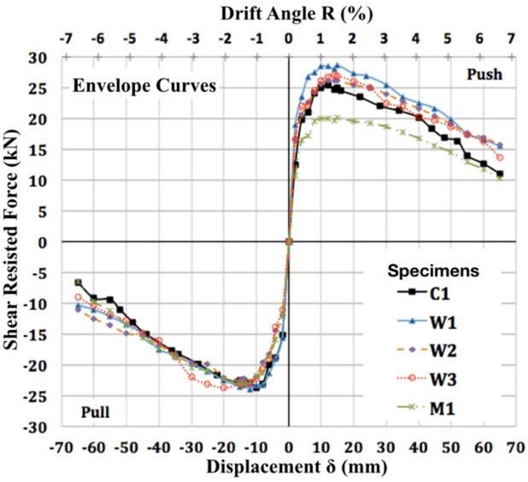

Fig. 7 Envelope curves of the hysteresis loops

4. Interpretation of the experimental results and the hysteretic behaviour of the specimens

The seismic behaviour of subassemblages W_1, W_2, W_3 and M_1 is subsequently evaluated using data acquired from the experimental equipment during testing. Thus, the efficiency and suitability of the examined types of welded rebars and of the mechanical splices of reinforcement in ensuring the ductile response of the columns were investigated by evaluating the percieved lateral strength, peak-to-peak stiffness and hysteretic energy dissipation capacity. Furthermore, the cyclic lateral performance of the subassemblages was compared to that of a control specimen (C_1) with continuous column reinforcement, tested by Kalogeropoulos and Tsonos (2019). For this purpose, the experimental results and the seismic behaviour of specimen C_1 are also discussed herein. The cyclic lateral response of all specimens is clearly reflected in the hysteresis loops and the envelope curves illustrated in Figs. 7 and 8. The material properties of subassemblages W_1, W_2, W_3 and M_1 are shown in Table 1. All specimens had the same details of reinforcement and were subjected to the same sequence of lateral displacement reversals.

All specimens exhibited a progressive slow-rate reduction of lateral strength in both cases of push half-cycles and pull half-cycles of the earthquake-type loading (see Figs. 7 and 8). The columns with welded rebars, W_1, W_2 and W_3, showed similar values of resisting shear forces throughout testing. The hysteresis loops' envelope curves of all specimens were similar in the case of pull half-cycles, while in the case of push half-cycles the column with mechanical splices of reinforcement, M_1, showed lower values of lateral strength than the columns with welded rebars, and the control specimen with continuous reinforcement, C_1 (see Fig. 7). This is attributed to the slippage of mechanically-spliced bars found on the side of the column which was under tension during the push half-cycles of the lateral displacement history. For drift angle, R, equal to 6.63 percent the lateral strength ratio values W_1/C_1, W_2/C_1, W_3/C_1 and M_1/C_1 for the push half-cycles equaled to 1.42, 1.42, 1.24 and 0.94, respectively. The corresponding ratio values for the pull half-cycles were

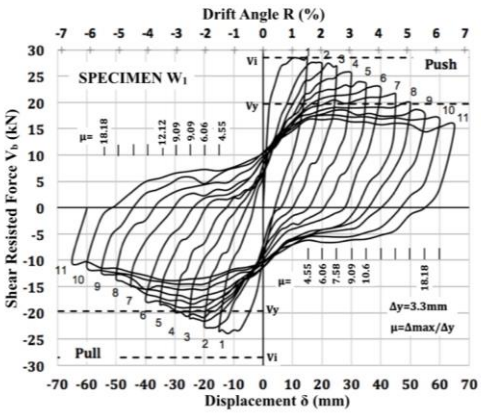

(a) Hysteresis loops of specimen W_1

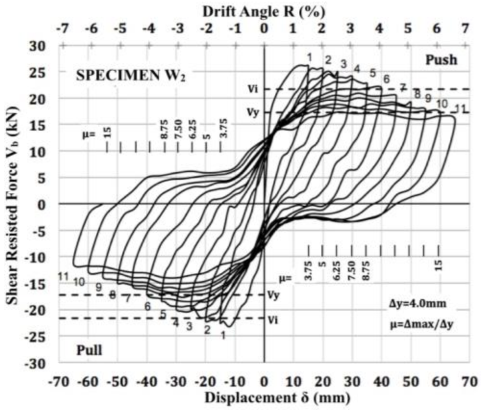

(b) Hysteresis loops of specimens W_2

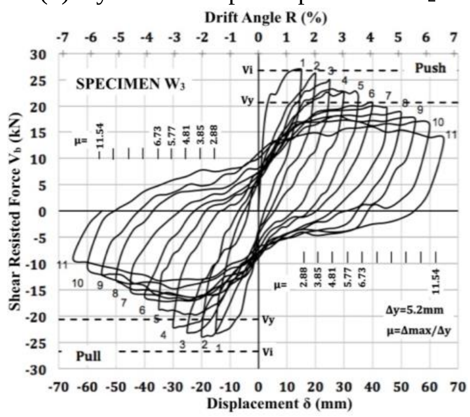

(c) Hysteresis loops of specimens W_3

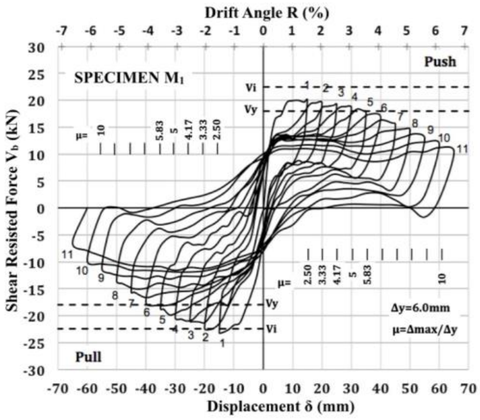

(d) Hysteresis loops of specimens M_1

Fig. 8 (a-d): Plots of shear resisted force-versus-displacement of the column subassemblages

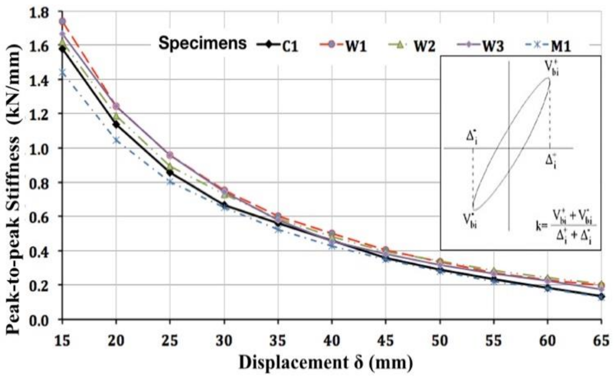

(a)

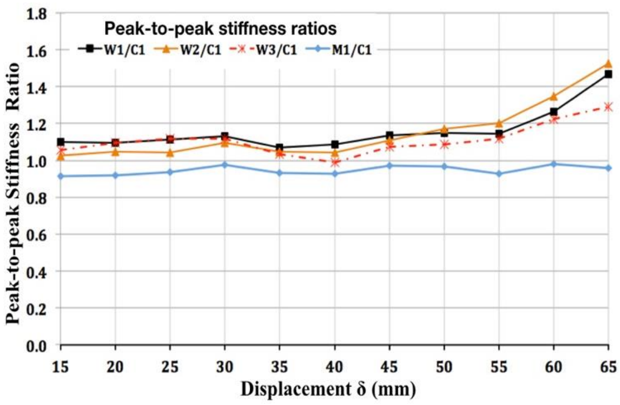

(b)

Fig. 9 Plots of (a) stiffness-versus-displacement and (b) stiffness ratios-versus-displacement of the column subassemblages (specimen C_1: Kalogeropoulos and Tsonos 2019)

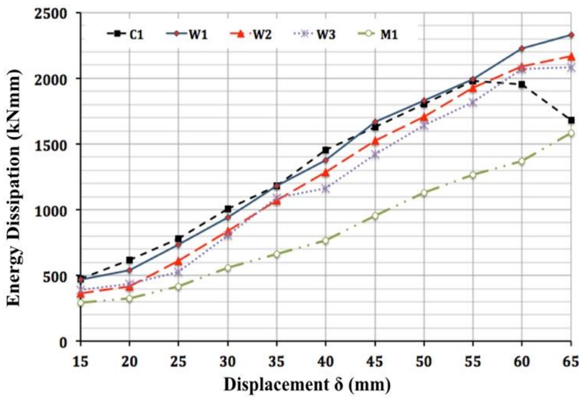

(a)

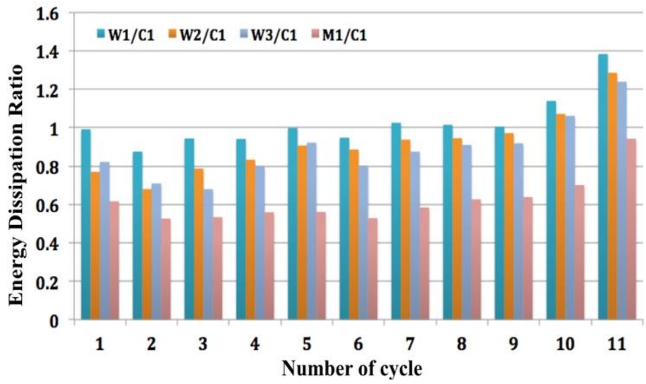

(b)

Fig. 10 Plots of: (a) Energy dissipation capacity-versus-displacement and (b) Energy dissipation ratios-versus-displacement of the column subassemblages. (specimen C_1: Kalogeropoulos and Tsonos 2019)

equal to 1.56, 1.68, 1.36 and 0.98, respectively. One notable outcome of the research was that the columns with welded rebars, W_1, W_2 and W_3, showed slightly increased values of lateral strength with respect to the control specimen with continuous reinforcing bars, C_1. One reason for this was that welding of the rebar was appropriately executed according to the provisions of the CSRTC (2008) and thus, failure of the welding was effectively precluded. Meanwhile, B500C steel reinforcement and C20/25 concrete were used in the case of column specimens W_1, W_2 and W_3, instead of S220 steel bars and concrete with compression strength of approximately 10MPa in the case of column C_1. Furthermore, the transverse reinforcement of W_1, W_2 and W_3 consisted of 8mm B500C closed ties with 135-degree hook ends spaced at 80mm, instead of 6mm S220 closed ties with 90-degree hook ends spaced at 200mm in the case of the control specimen C_1. As a result, buckling of the longitudinal reinforcement was ultimately prevented in the case of specimens W_1, W_2 and W_3 as opposed to column C_1.

The rate of peak-to-peak stiffness reduction during the cyclic loading was similar for all columns (see Fig. 9). Specimens W_1, W_2 and W_3 showed slightly increased values of peak-to-peak stiffness with respect to the control subassemblage C_1 and to the column with mechanical splices of reinforcement, M_1. For drift angle, R, equal to 6.63 percent the remained stiffness of the columns ranged from 8.55 percent (column C_1) to 12.72 percent (column W_2) of the corresponding initial values during the first cycle of loading. Moreover, at the end of the testing the stiffness ratios W_1/C_1, W_2/C_1, W_3/C_1 and M_1/C_1 equaled to 1.47, 1.53, 1.29 and 0.96, respectively (see Fig. 9(b)).

The column specimens with welded rebars, W_1, W_2 and W_3, exhibited dissipating hysteresis behaviour characterized by a continuous increase in energy dissipation values during testing. The latter were similar or even exceeded the corresponding values of the control specimen, C_1. The subassemblage with mechanical splices of reinforcement, M_1, also showed gradually incremental values of energy dissipated in the plastic hinge of the column, however, these values were lower than the corresponding ones of specimens W_1, W_2, W_3 and C_1. In particular, during the first cycle of loading the values of energy dissipation ratios W_1/C_1, W_2/C_1, W_3/C_1 and M_1/C_1 equaled to 0.99, 0.77, 0.82 and 0.615, respectively (see Fig. 10). For drift angle, R, equal to 6.63 percent the corresponding values equaled to 1.38, 1.29, 1.24 and 0.94. Therefore, it was clearly demonstrated that significant amount of seismic energy, similar to the amount of energy dissipated in the plastic hinge of the column with continuous reinforcement, C_1, was successfully dissipated in the plastic hinge region of columns W_1, W_2 and W_3. This was also reflected in the wide area of hysteresis loops of specimens W_1, W_2 and W_3. Due to a partial failure of mechanical splices of reinforcement in

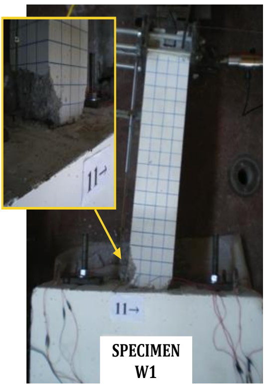

(a) Specimen W_1

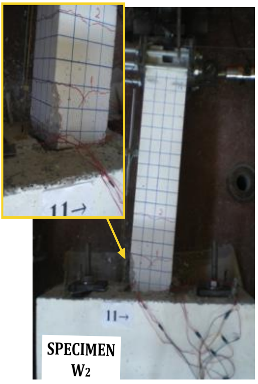

(b) Specimen W_2

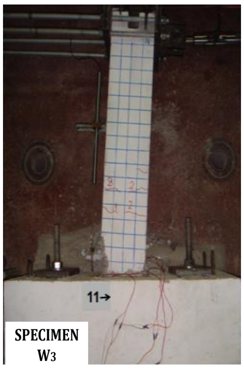

(c) Specimen W_3

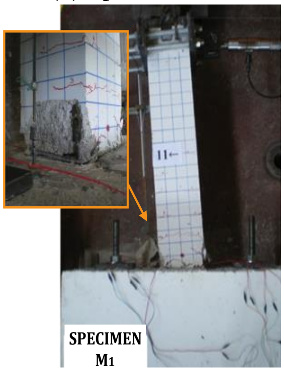

(d) Specimen M_1

Fig. 11 Failure mode of the column subassemblages

the case of specimen M_1, slipping of steel bars occurred. As a result, the area of the hysteretic loops and hence, the amount of energy dissipated were lower than in columns W_1, W_2, W_3 and C_1. Moreover, the slipping of steel bars had another adverse impact to the seismic behavior of column M_1, which was the increased influence of the P-Δ effect, with respect to specimens W_1, W_2, W_3 and C_1. The latter caused modest pinching of the hysteresis loops around the axes (see Fig. 8). After the seventh cycle of the earthquake-type loading (drift angle 4.59 percent) the values of the resisted shear force remained stable with the increase of lateral displacement. This was attributed to both minor slipping of the bars in the plastic hinge region, as well as to the narrowing of flexural cracks. In the case of specimen M_1, increased slipping of steel bars occurred on the one side of the column after the third push half-cycle of loading until the end of testing. On the other side of the column (pull half-cycles) the mechanical splices of reinforcement were satisfactory, while minor slipping of the bars occurred after the seventh pull half-cycle of loading.

Ultimately, the columns with welded rebars demonstrated a particularly ductile seismic response, due to the efficiency of the three examined types of SMAW applied. Meanwhile, the column with mechanical splices of reinforcement showed a slightly inferior cyclic performance due to the partial failure of the mechanical connection.

5. Monitoring of steel bar micro-strain

Monitoring of the steel strain value variations during the

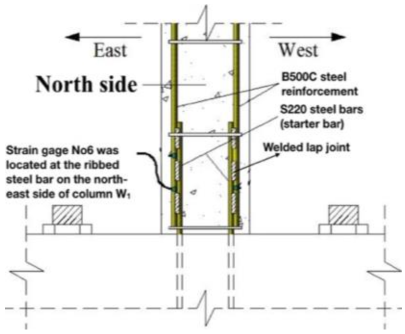

(a) Location of strain gauge No6 - Specimen W_1

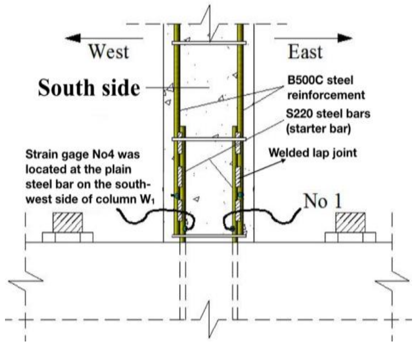

(b) Location of strain gauge No4 - Specimen W_1

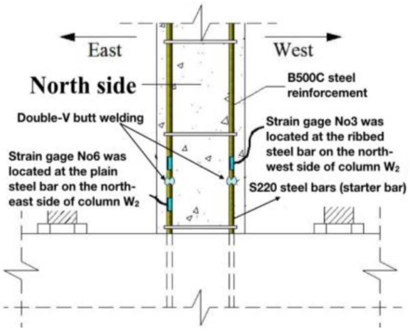

(c) Location of strain gauges No6 and No3 - Specimen W_2

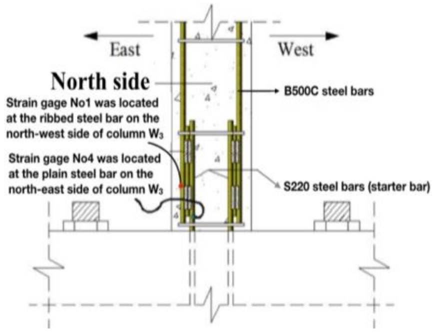

(d) Location of strain gauges No1 and No4 - Specimen W_3

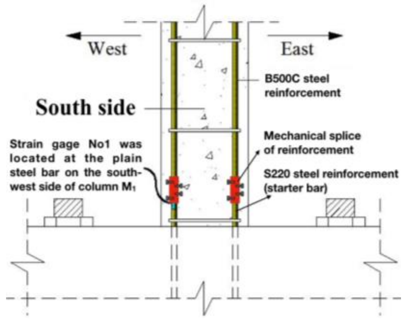

(e) Location of strain gauge No1 - Specimen M_1

Fig. 12 Location of strain gages

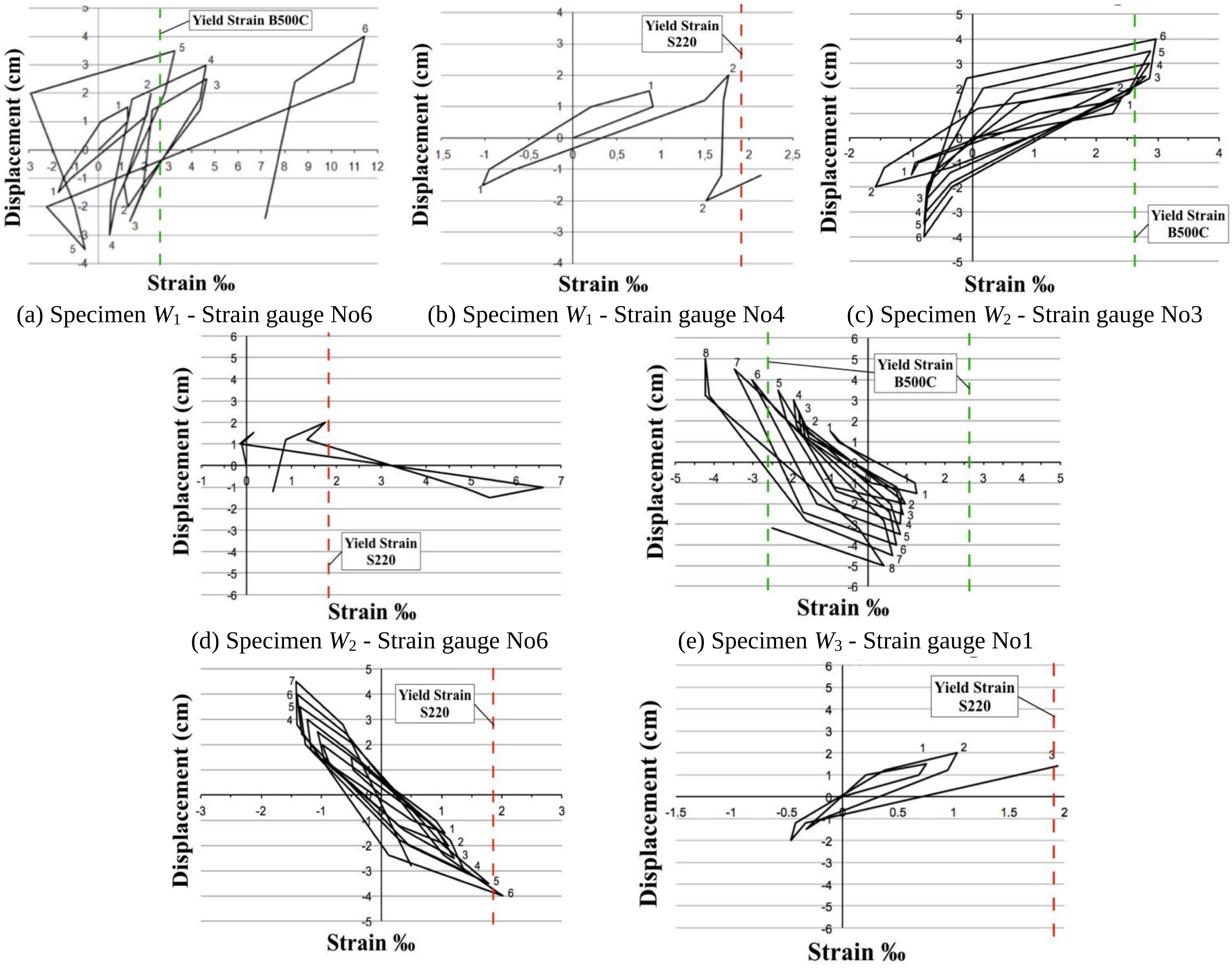

(a) Specimen W_1 - Strain gauge No6 (b) Specimen W_1 - Strain gauge No4 (c) Specimen W_2 - Strain gauge No3

(d) Specimen W_2 - Strain gauge No6 (e) Specimen W_3 - Strain gauge No1

(f) Specimen W_3 - Strain gauge No4 (g) Specimen M_1 - Strain gauge No1

Fig. 13 Plots of displacement-versus-strain

earthquake-type loading of the column subassemblages was achieved using electrical resistant strain gauges, which were attached to the bars. The exact location of each strain gauge is presented in Fig. 12, while in Fig. 13 the plots of the load point displacement-versus-strain of reinforcement are illustrated. The latter provided critical and valuable information about the columns' response, when subjected to inelastic cyclic lateral deformations. In particular, strain values which exceeded (in some cases significantly) the yield strain for both the cases of the plain S220 starter bars and the B500C column reinforcement were recorded during testing of all specimens (see Figs. 13(a)-(g)). Moreover, a continuous increase in maximum steel strain to post-yield values during consecutive cycles of loading was observed. The latter indicates the absence of bar slipping and ultimately, the ductile seismic response of the columns (Ehsani and Whight 1985). The opposite is true for stable or decreasing strain values, which reflect hysteresis deterioration due to the slippage of the bars, as long as buckling has not taken place. Therefore, both the SMAW of the rebars and the mechanical splices of reinforcement successfully prevented slipping of the bars, while allowing the development of the nominal flexural moment capacity of the columns (see Figs. 8 and 13). Thus, the specimens W_1, W_2, W_3 and M_1 performed in a ductile manner similar to that of the control specimen, C_1, with continuous column reinforcement (Kalogeropoulos and Tsonos 2019). This can also be observed by the failure mode of the specimens (see Fig. 11), which included a few hairline flexural cracks along the critical column height and the principal flexural crack at the columns' base. The latter was initially formed during the first cycle of the earthquake-type loading and subsequently dilated progressively during the incremental displacement reversals of the loading sequence.

6. Conclusions

Four cantilever column subassemblages of 1:1.5 scale were constructed and subjected to inelastic cyclic lateral displacements under constant axial loading. The efficiency and reliability of three types of welded rebars and of mechanical splices of reinforcement in preventing slipping of the bars and ensuring load transfer between the starter bars and the new column reinforcement, were evaluated. Moreover, the seismic behaviour of the column subassmblages was compared to the cyclic performance of a control specimen with continuous longitudinal reinforcement tested in a previous research work (Kalogeropoulos and Tsonos 2019). The following conclusions are drawn based on the experimental work presented herein:

• The shielded metal arc welding effectively prevented slippage of the columns' longitudinal reinforcement. In particular, both the examined types of welded lap joint, as well as the Double-V butt welding of rebar were equally satisfactory in ensuring yielding of reinforcement. The latter was confirmed from data acquired by the electrical resistant strain gauges, showing that yielding of both the starter bars and of the new column reinforcement was achieved.

• The welding of steel reinforcement was appropriately executed according to the recommendations of the CSRTC (2008). Due to the implementation of rigorous standards, failure of the welding was successfully precluded. Thus, all specimens with welded rebars (W_1, W_2 and W_3) exhibited a dissipating hysteresis behaviour. This was clearly reflected in the hysteresis loops of the columns. The latter were characterized by a continuous increase energy dissipation capacity and slow-rate of deterioration of lateral strength and peak-to-peak stiffness throughout testing. Moreover, owing to the low influence of the P-Δ effect, minor pinching around the axes in the hysteresis loops of the columns was observed.

• The lateral strength values of columns with the welded rebars, W_1, W_2 and W_3, were found to be slightly increased compared to the corresponding values of the control specimen with continuous reinforcing bars, C_1. This results from both the reinforcement details and the high quality of the welding and of the materials (concrete and steel) used in the case of columns W_1, W_2 and W_3 with respect to specimen C_1.

• The seismic behaviour of specimen with mechanical splices of reinforcement, M_1, was inferior to the performance of columns with welded rebars and to the performance of the control specimen C_1. This is attributed to the partial failure of the mechanical connection on the one side of the column. As a result, the hysteresis behaviour of M_1 was characterized by increased influence of the P-Δ effect.

• Thus, both methods could be successfully applied during the vertical extension of existing RC structures. Moreover, both methods could also be used as an alternative solution to improving load transfer between inadequately lap-spliced column reinforcing bars, instead of providing additional confinement to the plastic hinge region.

References

Aboutaha, R.S., Engelhardt, M.D., Jirsa, J.O. and Kreger, M.E. (1999), "Rehabilitation of shear critical concrete columns by use of rectangular steel jackets", *ACI Struct. J.*, **96**(1), 68-78.

Apostolopoulos, C.A., Michalopoulos, D. and Dimitrov, L. (2008), "The impact of corrosion on the mechanical behavior of welded splices of reinforcing steel S400 and B500C", *J. Mater. Eng. Perf.*, **17**(1), 70-79. https://doi.org/10.1007/s11665-007-9147-7.

ASTM E 415-08 (2008), Standard Test Method for Atomic Emission Vacuum Spectrometric Analysis of Carbon and Low-Alloy Steel, West Conshohocken, PA, USA.

Chai, H.Y., Priestley, M.N.J. and Seible, F. (1991), "Seismic retrofit of circular bridge columns for enhanced flexural performance", *ACI Struct. J.*, **88**(5), 572-584.

Chalioris, C. and Bantilas, K. (2017), "Shear strength of reinforced concrete beam-column joints with crossed inclined bars", *Eng. Struct.*, **140**, 241-255. https://doi.org/10.1016/j.engstruct.2017.02.072.

Choi, E., Chung, Y.S., Park, K. and Jeon, J.S. (2013), "Effect of steel wrapping jackets on the bond strength of concrete and the lateral performance of circular rc columns", *Eng. Struct.*, **48**, 43-54. https://doi.org/10.1016/j.engstruct.2012.08.026.

CSRTC (2008), New Code of Steel Reinforcement Technology for Concrete, Athens, Greece.

Daudey, X. and Filiatrault, A. (2000), "Seismic evaluation and retrofit with steel jackets of reinforced concrete bridge piers detailed with lap-splices", *Can. J. Civil Eng.*, **27**(1), 1-16. https://doi.org/10.1139/l99-029.

Durrani, A.J. and Wight, J.K. (1987), "Earthquake resistance of reinforced concrete interior connections including a floor slab", *ACI J. Proc.*, **84**(84-S42), 400-406.

Ehsani, M.R. and Wight, J.K. (1985), "Effect of transverse and slab on behavior of reinforced concrete beam-to-column connections", *ACI J. Proc.*, **82**(82-17), 188-195.

Ehsani, M.R. and Wight, J.K. (1985), "Exterior reinforced concrete beam-to-column connections subjected to earthquake - type loading", *ACI J. Proc.*, **82**(4), 492-499.

El Gawady, M., Endeshaw, M., McLean, D. and Sack, R. (2010), "Retrofitting of rectangular columns with deficient lap splices", *J. Compos. Constr.*, **14**(1), 22-35. https://doi.org/10.1061/(ASCE)CC.1943-5614.0000047.

EN 1998-1-1 Eurocode 2 (2004), Design of Concrete Structures. Part 1-1, General Rules and Rules for Buildings, 224.

EN 1998-1 Eurocode 8 (2004), Design of Structures for Earthquake Resistance. Part 1: General Rules, Seismic Actions and Rules for Buildings, Stage 51, 229.

Haber, Z.B., Saiid Saiidi, M. and Sanders, D.H. (2014), "Seismic performance of precast columns with mechanically spliced column-footing connections", *ACI Struct. J.*, **111**(1-6), 1-12.

Haber, Z.B., Saiid Saiidi, M. and Sanders, D.H. (2015), "Behavior and simplified modelling of mechanical reinforcing bar splices", *ACI Struct. J.*, **112**(2), 179-188.

Hakuto, S., Park, R. and Tanaka, H. (2000), "Seismic load tests on interior and exterior beam-column joints with substandard reinforcing details", *ACI Struct. J.*, **97**(1), 11-25.

Issar, A.C. and Nasr, A. (2006), "An experimental study of welded splices of reinforcing bars", *Build. Environ. J.*, **41**(10), 1394-1405. https://doi.org/10.1016/j.buildenv.2005.05.025.

Kakaletsis, D., David, K. and Karayannis, C. (2011), "Effectiveness of some conventional seismic retrofitting techniques for bare and infilled R/C frame", *Struct. Eng. Mech.*, **39**(4), 499-520. https://doi.org/10.12989/sem.2011.39.4.499.

Kalogeropoulos, G. and Tsonos, A.D. (2014), "Effectiveness of r/c jacketing of substandard r/c columns with short lap splices", *Struct. Monit. Maint.*, **1**(3), 273-292. https://doi.org/10.12989/smm.2014.1.3.273.

Kalogeropoulos, G. and Tsonos, A.D. (2019), "Improvement of the cyclic response of RC columns with inadequate lap splices - Experimental and analytical investigation", *Earthq. Struct.*, **16**(3), 279-293. https://doi.org/10.12989/eas.2019.16.3.279.

Karayannis, C. (2015), "Mechanics of external RC beam-column joints with rectangular spiral shear reinforcement: experimental verification", *J. Meccanica*, **50**(3), 311-322. https://doi.org/10.1007/s11012-014-9953-6.

Karayannis, C. and Golias, E. (2018), "Full scale tests of RC joints with minor to moderate seismic damage repaired using C-FRP sheets", *Earthq. Struct.*, **15**(6), 617-627. https://doi.org/10.12989/eas.2018.15.6.617.

Lee, S.J., Lee, D.H., Kim, K.S., Oh, J.Y., Park, M.K. and Yang, I.S. (2013), "Seismic performances of RC columns reinforced with screw ribbed reinforcements connected by mechanical splice", *Comput. Concete*, **12**(2), 131-149. https://doi.org/10.12989/cac.2013.12.2.131.

Pampanin, S., Bolognini, D. and Pavese, A. (2007), "Performance-based seismic retrofit strategy for existing reinforced concrete frame systems using fiber-reinforced polymer composites", *J. Compos. Constr.*, 211-226. https://doi.org/10.1061/(ASCE)1090-0268(2007)11:2(211).

Paulay, T. (1982), "Lapped splices in earthquake-resisting columns", *ACI Struct. J.*, 458-469.

Paulson, C. and Hanson J.M. (1991), "Fatigue behavior of welded and mechanical splices in reinforcing steel", Final Report, Chicago and Northbrook, Illinois, USA.

Pavese, A., Bolognini, D. and Peloso, S. (2004), "FRP seismic retrofit of RC square hollow section bridge piers", *J. Earthq. Eng.*, **8**(1), 225-250.

Priestley, M.J.N., Seible, F. and Calvi, G.M. (1996), *Seismic design and Retrofit of Bridges*, John Willey and Sons, New York, NY, USA.

Tazarv, M. and Saiid Saiidi, M. (2016), "Seismic design of bridge columns incorporating mechanical bar splices in plastic hinge regions", *Eng. Struct.*, **124**, 507-520. https://doi.org/10.1016/j.engstruct.2016.06.041.

CC